


High-throughput analysis of T cell–monocyte interaction in human tuberculosis

M. Habtamu ^{*,†}, G. Abrahamsen,^{*}
A. Aseffa,[†] E. Andargie,[†] S. Ayalew,[†]
M. Abebe[†] and A. Spurkland^{*}

^{*}Department of Molecular Medicine, Institute of Basic Medical Sciences, University of Oslo, Oslo, Norway, and [†]Armauer Hansen Research Institute, Addis Ababa, Ethiopia

Accepted for publication 19 April 2020

Correspondence: A. Spurkland, Department of Molecular Medicine, Institute of Basic Medical Sciences, University of Oslo, Oslo, Norway.

E-mail: anne.spurkland@medisin.uio.no

M. Habtamu, Department of Molecular Medicine, Institute of Basic Medical Sciences, University of Oslo, Oslo, Norway.

E-mail: mekonnen.meseret@gmail.com

Summary

The lack of efficient tools for identifying immunological correlates of tuberculosis (TB) protection or risk of disease progression impedes the development of improved control strategies. To more clearly understand the host response in TB, we recently established an imaging flow cytometer-based *in-vitro* assay, which assesses multiple aspects of T cell–monocyte interaction. Here, we extended our previous work and characterized communication between T cells and monocytes using clinical samples from individuals with different TB infection status and healthy controls from a TB endemic setting. To identify T cell–monocyte conjugates, peripheral blood mononuclear cells (PBMC) were stimulated with ds-Red-expressing *Mycobacterium bovis* bacille Calmette–Guérin or 6-kDa early secreted antigenic target (ESAT 6) peptides for 6 h, and analyzed by imaging flow cytometer (IFC). We then enumerated T cell–monocyte conjugates using polarization of T cell receptor (TCR) and F-actin as markers for synapse formation, and nuclear factor kappa B (NF- κ B) nuclear translocation in the T cells. We observed a reduced frequency of T cell–monocyte conjugates in cells from patients with active pulmonary tuberculosis (pTB) compared to latent TB-infected (LTBI) and healthy controls. When we monitored NF- κ B nuclear translocation in T cells interacting with monocytes, the proportion of responding cells was significantly higher in active pTB compared with LTBI and controls. Overall, these data underscore the need to consider multiple immunological parameters against TB, where IFC could be a valuable tool.

Keywords: cell activation, monocyte, T cell

Introduction

Tuberculosis (TB) remains one of the major global public health threats due to its high morbidity and mortality, especially in the developing world [1]. The absence of an efficacious vaccine is one of the key challenges in the control of TB. The delay in developing more effective vaccines and better control strategies is partially attributed to the lack of suitable technologies for defining immune correlates of TB protection and risk of disease progression [2].

Indeed, earlier studies have shown that host protection against TB relies mainly on T helper type 1 (Th1) cells [3,4]. Thus, phenotypical and functional characterization of the TB-specific Th1 response has been considered as

a potential end-point parameter for assessing vaccine and infection-induced immune response. Nonetheless, the results reported from such studies are inconsistent and contradictory. It has been shown that the levels of Th1 responses inducing secretion of interferon (IFN)- γ do not correlate with host protection [5–8]. In fact, latent TB-infected (LTBI) individuals whose T cells produce greater amounts of IFN- γ were more likely to develop active disease than those with weaker responses [9,10].

The host immune response against *Mycobacterium tuberculosis* (*Mtb*) is a complex process dependent upon a well-co-ordinated interplay between innate and adaptive immunity [11–13]. Innate immunity is the first line of defense

following antigen exposure. The ability of the innate immune response to rapidly recognize and respond is one of the determining factors for resistance to the establishment of sustained *Mtb* infection or active disease development [14].

The multi-faceted biological interaction between *Mtb* and host cells needs to be taken into account in the search for correlates of immune protection. This can be achieved by concurrently characterizing T cell–antigen-presenting cell (APC) interaction in the panel of functional assays. Monocytes are among the primary cells that are attracted to the affected tissue early following *Mtb* infection [15,16], and play key roles in modulating multiple aspects of host immunity as precursors of macrophages and dendritic cells [17]. It has also been acknowledged that monocytes may also function as APC, bridging innate and adaptive immune responses [18,19].

Pathogen recognition and subsequent T cell activation requires efficient interaction between T cells and APCs. Upon cognate peptide major histocompatibility complex (pMHC) presentation, a highly organized and dynamic molecular structure, named an ‘immunological synapse’ (IS) is formed at the T cell–APC contact site [20,21]. IS formation is dependent upon cytoskeletal and membrane proteins reorganization towards the contact site, where polarization of T cell receptor (TCR) and F-actin are among the key elements [22,23].

T cell–APC interaction initiates intracellular signaling cascades within the T cell, which results in the activation and nuclear translocation of transcription factors. Nuclear factor kappa-B (NF- κ B) is a family of transcription factors that regulate genes involved in various aspects of host immune response (reviewed in [24,25]). Hence, assessing immunological network signatures on the basis of T cell–APC interaction with established synapse and NF- κ B nuclear translocation in responding T cells could provide valuable insight in defining immune protection against TB.

Our group has taken advantage of this and recently established an IFC-based *in-vitro* assay using healthy donor human PBMC with the potential to be used in TB biomarker discovery [26]. In the present study, we have employed this method on clinical samples from patients with active pulmonary TB (pTB), LTBI and healthy endemic controls (EC) and investigated T cell–monocyte conjugates with polarized TCR and F-actin as markers for synapse formation. In addition, we assessed if our system can detect differences in downstream signaling events in T cells among study cohorts by monitoring NF- κ B nuclear translocation.

Materials and methods

Study participants

Study participants were recruited prospectively from four health centers in Addis Ababa, Ethiopia from March

2015 to July 2016. Clinically and bacteriologically confirmed patients with active pulmonary TB were recruited prior to initiation of anti-TB treatment. For the control group, apparently healthy participants were recruited from Voluntary Counselling and Testing (VCT) clinics for HIV from the same study sites as TB patients. All participants aged 18–65 years, tested HIV seronegative, free of other concomitant diseases and not on immune modulatory treatment were included in the study. Individuals with LTBI and healthy EC were classified on the basis of QuantiFERON-TB Gold In-Tube assay results.

The study was approved by national Research Ethics Review committees in Ethiopia (AAERC/P002/15) and Norway (2015/136/REK sør-øst), and conducted in accordance with the Declaration of Helsinki. Written informed consent was obtained from each participant prior to recruitment and sample collection.

Antibodies, reagents and antigens

Antibodies used in this study included: anti-CD3-fluorescein isothiocyanate (FITC) (clone UCHT1, cat. no. 21620033; ImmunoTools, Friesoythe, Germany), anti-CD14-allophycocyanin (clone MEM-15, cat. no. 21279146, ImmunoTools), rabbit polyclonal immunoglobulin (Ig)G (C-20) anti-human NF- κ B primary antibody (cat. no. SC-372R; Santa Cruz Biotechnology, Santa Cruz, CA, USA), Alexa Fluor 594, goat anti-rabbit IgG (H⁺L) secondary antibody (cat. no. R37117; Molecular Probes, Invitrogen, Carlsbad, CA, USA), biotin-labeled phalloidin (cat. no. B7474; ThermoFisher, Fremont, CA, USA), streptavidin APC e-fluor 780 (cat. no. 47-4317-82; ThermoFisher) and 4',6-diamidino-2-phenylindole (DAPI) nuclear stain (cat. no. 00-4959-52; ThermoFisher); RPMI-1640 complete medium supplemented with 10% fetal calf serum (FCS), 100 units/ml penicillin, 100 μ g/ml streptomycin, 1 M HEPES buffer solution, 100 mM sodium-pyruvate, minimum essential medium non-essential amino acids (MEM NEAA) (\times 100) (all from GIBCO, Life Technologies, Carlsbad, CA, USA) and 2-mercaptoethanol (Sigma, St Louis, MO, USA). Mycobacterial antigens used included: the 6-kDa early secreted antigenic target (ESAT-6) (15mer overlapping custom made peptides, Genscript, a kind gift from Dr Even Fossum) and ds-Red fluorescent protein-expressing bacille Calmette–Guérin (BCG) strain Myc3305 (provided by Dr Brigitte Gicquel) [27].

Cell culture and staining

Up to 20 ml venous blood was collected in ethylenediamine tetraacetic acid (EDTA)-containing tubes from all study cohorts. Peripheral blood mononuclear cells (PBMC) were isolated by density gradient centrifugation using Lymphoprep (Axis-Shield PoC AS, Oslo, Norway), and

cryopreserved in RPMI-1640 with 10% dimethylsulfoxide (DMSO) and 20% fetal calf serum (FCS). Prior to setting up experiments, PBMC were thawed, washed and resuspended in RPMI-1640 complete medium supplemented with 10% FCS, and allowed to rest overnight at 37°C and 5% CO₂ [28]. PBMC with a concentration of 1×10^6 cells/ml were then incubated with ESAT 6 peptides (2 µg/ml) or ds-Red fluorescent protein-expressing BCG [3×10^6 colony-forming units (CFU)/ml] at 37°C and 5% CO₂ for 6 h. PBMC incubated in culture medium alone under the same conditions were used as unstimulated control. Cells were harvested after careful scraping, and then transferred to microcentrifuge tubes for fluorochrome staining.

Harvested cells were washed once with cold fluorescence activated cell sorter (FACS) buffer (2% FCS, 0.1% sodium azide in PBS). Prior to anti-CD3 and anti-CD14 surface staining, cells were then treated with 10% heat-inactivated human serum in FACS buffer for 10 min to block non-specific staining. For detection of NF-κB, cells were fixed in 2% paraformaldehyde (PFA) for 10 min at room temperature and incubated with 0.1% Triton-X permeabilization buffer (Sigma) at 4°C for 5 min. Cells were then incubated with rabbit anti-human NF-κB primary antibody for 30 min followed by AF594-labeled goat anti-rabbit secondary antibody together with DAPI nuclear stain for another 30 min, on ice and in the dark. F-actin was detected by incubating PFA fixed cells with biotin-tagged phalloidin for 30 min followed by incubation with APC-eFluor 780-labeled streptavidin for another 30 min. A schematic overview of the experimental set-up is outlined in Fig. 1a.

ImageStream^X data acquisition

An ImageStream^X MkII Imaging flow cytometer (Amnis Corporation, Seattle, WA, USA), with a 12-channel system equipped with four lasers and ASSIST-calibrated, was used for data acquisition (Amnis Corporation). Up to 150 000 events were acquired for each sample with $\times 40$ magnification using INSPIRE software (Amnis Corporation). Images acquired include bright-field (channels 01 and 09), CD3-FITC (channel-02), ds-Red BCG (channel-03), NF-κB AF594 (channel-04), DAPI (channel-07), CD14-allophycocyanin (channel-11) and phalloidin-APC-eFluor 780 (channel-12). Cellular events were identified by setting a gate using a scatter-plot that allowed discriminating cells from speed beads, which is used as an internal calibrator for the machine. The gated cells were plotted as a histogram to collect only DAPI-positive events. Single-color-stained cells were acquired in every experiment with all the lasers 'on' and the bright-field illumination and scatter lasers 'off', which is used to create a compensation matrix and correct spectral overlap.

Imaging flow cytometry data analysis

The ImageStream^X data were analyzed using the ImageStream^X Data Exploration and Analysis Software (IDEAS) version 6.1 (Amnis Corporation) after spectral compensation. The hierarchical gating and analysis template was set up once and used throughout the experiment (Fig. 1b). Briefly, cellular events in camera focus were selected on the basis of the 'Gradient RMS' feature. Following this, the bright-field 'aspect ratio' *versus* 'area' was plotted to differentiate cellular aggregates and single cells [29,30]. The individual 'object' mask was generated to identify T cells and monocytes based on CD3-FITC and CD14-allophycocyanin fluorescence intensity, respectively.

Two cell conjugates were identified from cellular aggregates on the basis of low 'nuclear aspect ratio intensity' and two cell nuclear content (DAPI signal). Once events with two cell nuclear content were identified, those adjacent with 'one T cell' were gated on the basis of high 'CD3 aspect ratio intensity'. This subpopulation was plotted further to identify events of 'one T cell' conjugated with 'one monocyte' based on high 'CD14 aspect ratio intensity'. Eventually, T cell–monocyte conjugates with established synapse were determined by assessing polarization of TCR and F-actin at the contact site using the 'interface' masking tool. A histogram plot quantified the degree of TCR and F-actin polarization by calculating the average fluorescent signals of CD3 and phalloidin, respectively, within the T cell side of respective 'interface' masks as a ratio to the average fluorescent signal of the whole T cell [29,30].

The T cell–monocyte conjugate subpopulation was further characterized by plotting against ds-Red BCG fluorescent intensity within the conjugating monocyte, gated in the histogram as ds-Red-positive (ds-Red⁺) or ds-Red-negative (ds-Red⁻) conjugates. NF-κB nuclear translocation in T cells was assessed by applying the 'similarity' feature on IDEAS software used to generate 'morphology' mask based on the nuclear image. 'Similarity score' was assigned for each cell based on pixel intensity values of the DAPI and NF-κB images within the nuclear area of each T cell [26,31]. A histogram was plotted for each sample to determine the similarity score distribution (Fig. 1b, vii).

Statistical analysis

All graphs and statistical analyses were performed using GraphPad Prism software version 6.01 for windows (GraphPad Software, La Jolla, CA, USA; www.graphpad.com). The Kruskal–Wallis test followed by Dunn's multiple comparisons was used to compare differences among the three study groups. For matched data comparing two data sets, Wilcoxon's matched-pairs signed-rank test, and for more than two groups, Friedman's test with Dunn's multiple comparisons, was used. Statistical significance was achieved when $P < 0.05$.

Result

Characteristics of study participants

Forty-two treatment-naive smear-positive pulmonary tuberculosis (pTB) cases [mean ± standard deviation (s.d.), age = 28.2 ± 11 years, men/women = 23/19] and 76 apparently healthy individuals were recruited. The apparently

healthy participants were further classified based on the IFN-γ release assay [QuantiFERON-TB Gold (QFT®)] result: 33 (43.4%) were QFT-positive [mean ± s.d., age = 32 ± 10.3 years, men/women = 13/20] were considered as LTBI individuals while the remaining 43 (56.6%) were QFT-negative [mean ± s.d., age = 30.8 ± 10.8 years, men/women = 10/33] and were grouped as healthy EC (Table 1).

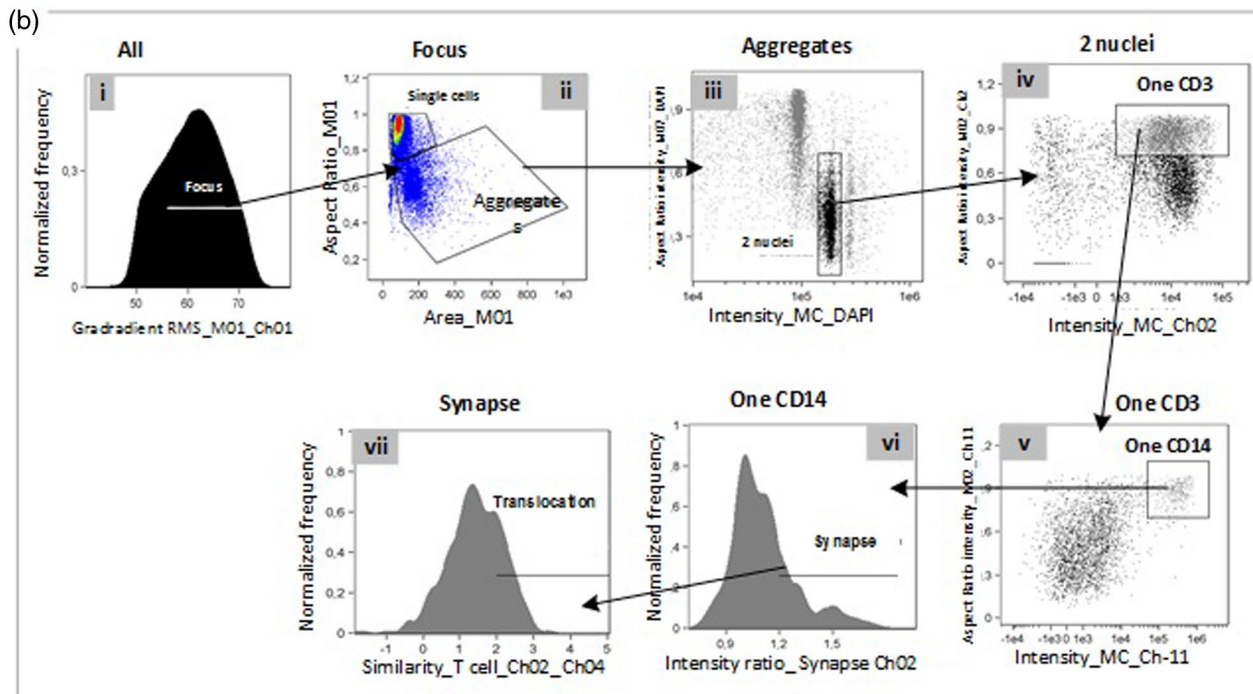
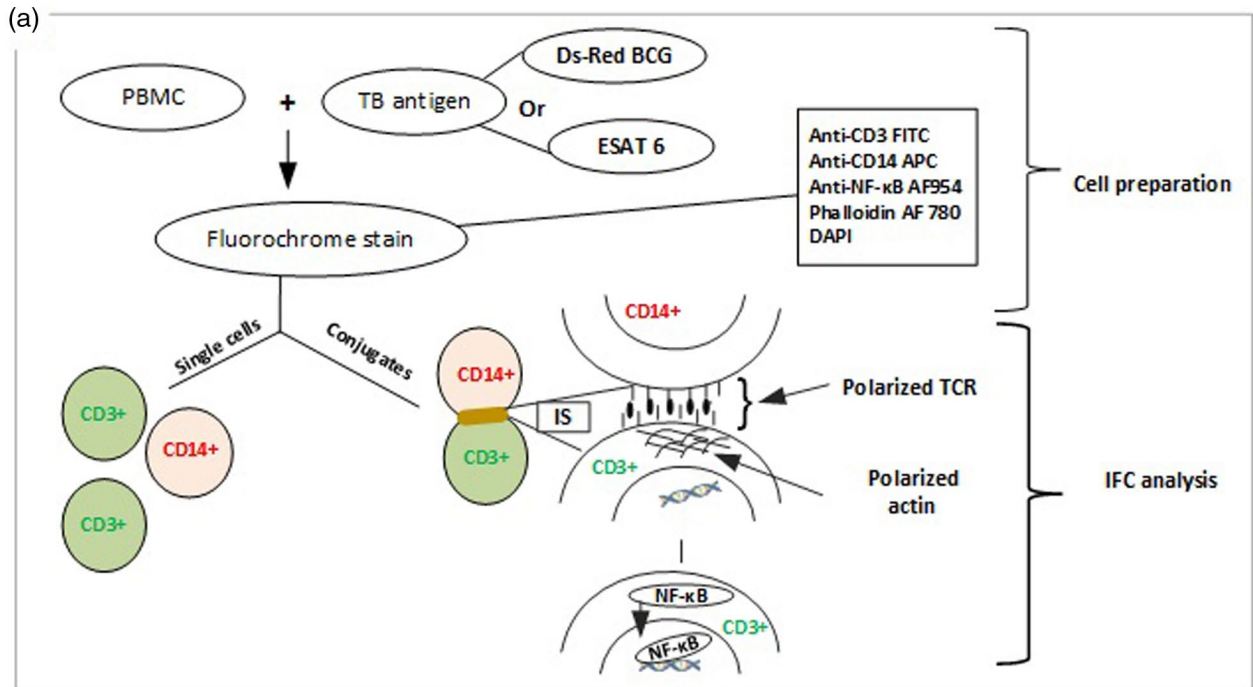


Fig. 1. Overview of experimental setup and gating strategy. (a) Schematic illustration describing cell preparation and imaging flow cytometer (IFC) analysis. Peripheral blood mononuclear cells (PBMC) from participants with active pulmonary tuberculosis disease (pTB), latent TB infection (LTBI) and healthy endemic controls (EC) were stimulated with ds-Red-expressing bacille Calmette–Guérin (BCG) or early secreted antigen 6 kilodaltons (ESAT 6) for 6 h. Fluorochrome-stained cells were then analyzed by IFC to identify CD3⁺ T cells and CD14⁺ monocytes. Cellular conjugates of single T cell with one monocyte were identified on the basis of CD3 and CD14 fluorescent signal. Polarization of T cell receptor (TCR) and F-actin (phalloidin AF780) were used as markers for immunological synapse formation at the contact site between the two cells. Nuclear factor kappa B (NF- κ B) nuclear localization was also assessed in CD3⁺ T cells. (b) Gating strategy applied to identify parameters of interest as follows: after acquiring events in camera focus (i), single cells and cellular aggregates were gated based on area *versus* aspect ratio (ii). Cell–cell conjugates with two nuclei were then identified on the basis of 4',6-diamidino-2-phenylindole (DAPI) intensity and lower aspect ratio of DAPI (iii). Those with 'one CD3⁺ cell' conjugated with 'one other cell' (iv) and 'one CD3⁺ cell' conjugated with 'one CD14⁺ cell' (v) were identified based on intensities of CD3-fluorescein isothiocyanate (FITC) and CD14-allophycocyanin, respectively. Subpopulations of 'one CD3⁺ cell' conjugated with 'one CD14⁺ cell' with synapse at the interface (vi). Of those conjugates with synapse, 'one CD3⁺ cell' conjugated with 'one CD14⁺ cell' displaying NF- κ B nuclear translocation have also been enumerated based on pixel intensity values of the DAPI and NF- κ B images for each target cell (vii).

Elevated monocyte-to-lymphocyte ratio in patients with active pTB

Studies have shown that the relative proportions of myeloid and lymphoid cells is associated with the extent of TB disease [32,33]. As these studies used transcriptomic or differential hematology analysis, we first aimed to validate whether our system was able to quantify the relevant T cell and monocyte populations prior to antigen stimulation based on CD3 and CD14 surface expression, respectively. A sample dot-plot of the gated single cell population showing CD3⁺ and CD14⁺ subpopulations of cells analyzed by IFC is presented in Fig. 2a. As shown in quantitative scatter-plots, the frequency of CD14⁺ monocyte was higher in patients with active pTB (Fig. 2b) while that of the CD3⁺ T cells was reduced in this study group compared to LTBI individuals and healthy EC (Fig. 2c). Consequently, the monocyte-to-T cell ratio was elevated in patients with active pTB compared to the control groups (Fig. 2d).

Fewer antigen-induced T cell–monocyte conjugates in PBMC from patients with active pTB

It has long been established that an immunological synapse (IS) is a specialized structure where sustained target–effector cell engagement and TCR signaling occur, an event which is required for proper activation and effector function of the responding T cells [22,23]. This is governed by localized intracellular signaling that leads to reorientation of cytoskeletal and membrane proteins, including F-actin, TCR and cell signaling molecules, towards the T cell–APC contact site [20,34]. In the present study, we stimulated PBMC of patients with active pTB, LTBI individuals and healthy EC with ESAT 6 or ds-Red-expressing BCG (BCG) and the extent of T cell–monocyte conjugate formation with synapse was assessed. Conjugates were identified by applying the gating strategy presented in Fig. 1b. Conjugates with established synapse were identified on the basis of polarized CD3/TCR and F-actin at the interface between 'one T cell' and 'one monocyte' (Fig. 3a, last column, upper panel, as indicated by white arrows). Having found that

Table 1. Characteristics of study cohorts: active pulmonary TB (pTB), latent TB infection (LTBI) or endemic controls (EC)

	LTBI		
	pTB (<i>n</i> = 42)	(<i>n</i> = 33)	EC (<i>n</i> = 43)
Age, years			
Mean (\pm s.d.), range	28.2 (11.0), 17–64	32 (10.3), 18–55	30.8 (10.8), 15–58
Gender			
Male (female)	23 (19)	13 (20)	10 (33)
QuantiFERON [®] -TB Gold			
Negative	–	0	43 (56.6%)
Positive	–	33 (43.4%)	0

patients with active pTB displayed increased frequencies of CD14⁺ monocytes, we would expect more conjugates to be identified in this study group. However, comparison between the study cohorts revealed a reduced frequency of T cell–monocyte conjugates with synapse in PBMC from patients with active pTB compared to the control groups (Fig. 3b).

Patients with active pTB had higher frequency of responding T cells displaying NF- κ B nuclear translocation

Once we had identified T cell–monocyte conjugates with established synapse, we moved on to assess its impact in the responding T cells on the basis of TB antigen-induced NF- κ B nuclear translocation (Fig. 4). NF- κ B and DAPI images along with their composites are displayed as a representative image gallery in Fig. 4a. Antigen-induced cytoplasmic-to-nuclear translocation of NF- κ B was monitored in T cells by applying the 'similarity score' feature, which quantifies the correlation of nuclear (DAPI) and NF- κ B image pixel intensities at a single cell level [26,31]. We first examined whether there was a difference in the extent of antigen-induced NF- κ B nuclear translocation among single T cells compared to those T cells conjugated with monocytes of the same sample. As expected, T cells that were engaged with monocytes as

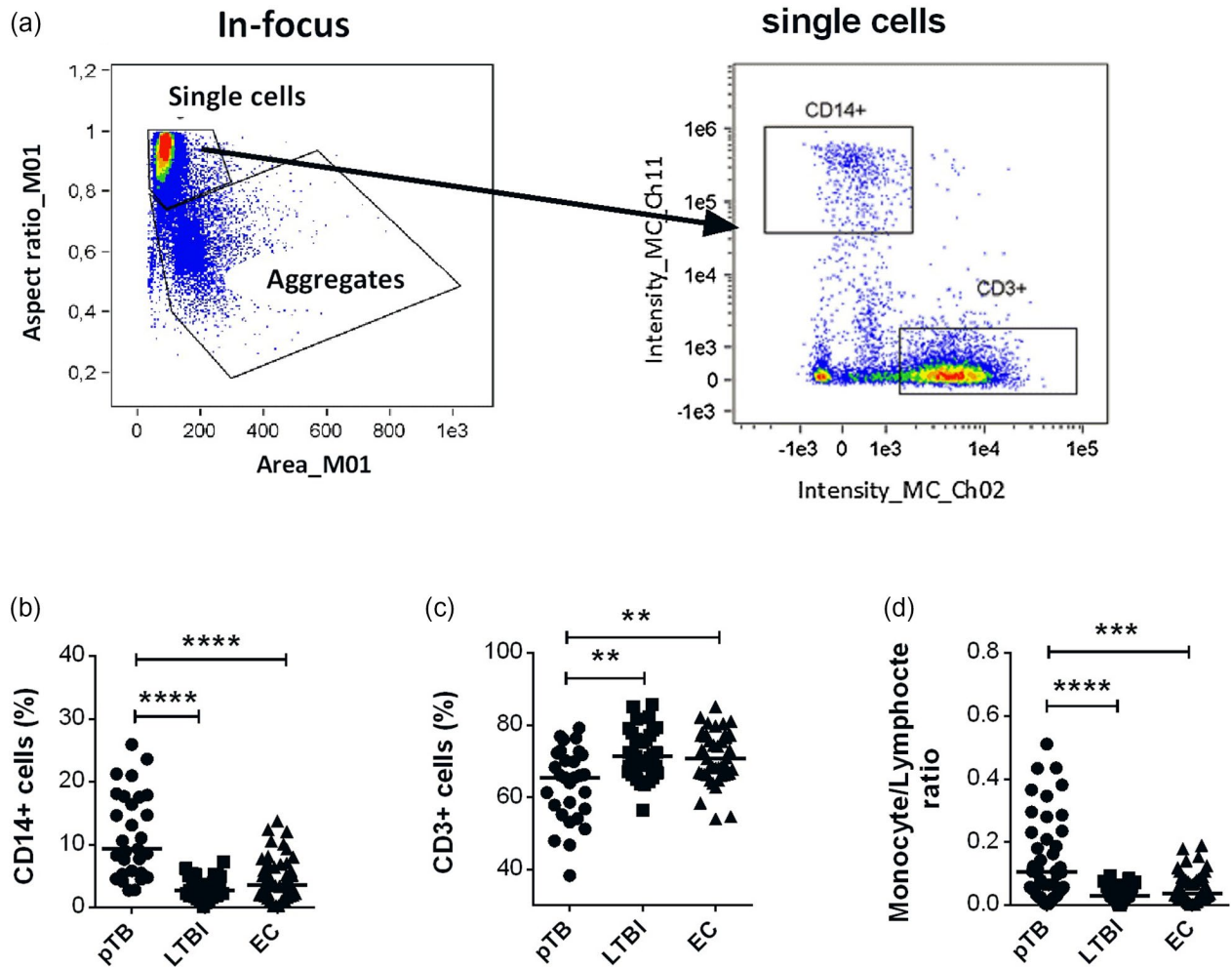


Fig. 2. Proportion of target cell population in peripheral blood mononuclear cells (PBMC) prior to stimulation. PBMC of patients with active pulmonary tuberculosis disease (pTB), latent TB infection (LTBI) individuals and endemic controls (EC) were stained for selected T cell and monocyte markers prior to stimulation with TB antigen. (a) Representative scatter-plot showing distribution of CD3⁺ and CD14⁺ subpopulations of all single cells gated from in-focus events. (b) Proportion of CD14⁺ monocytes, (c) CD3⁺ T cells and (d) monocyte-to-T cell ratio among pTB, LTBI and EC groups. Each dot represents frequency of individual patients with active pTB (circles), LTBI individuals (squares) and EC (triangles). Graphs are presented as scatter dot-plots and horizontal bars indicate median values in each group. Kruskal–Wallis test with Dunn’s multiple comparison was used to compare median differences among study cohorts: ** $P < 0.01$; *** $P < 0.001$; **** $P < 0.0001$.

conjugates and had formed a synapse displayed increased NF- κ B nuclear translocation compared to single T cells (Fig. 4b). Of note, both BCG and ESAT 6 stimulation induced NF- κ B nuclear translocation in T cell conjugates more frequently than that observed in spontaneously formed conjugates of unstimulated cells (Supporting information, Fig. S1). We then determined whether T cells from the three study cohorts responded differently. Although, as already presented in Fig. 3b, fewer conjugates were identified in cells from patients with active pTB, the T cells that were engaged with monocytes displayed NF- κ B nuclear translocation more frequently in this study

group than T cells from LTBI individuals and healthy EC (Fig. 4c).

Altered processing of BCG in monocytes from patients with active pTB

Culturing human PBMC together with ds-Red fluorescent protein-expressing BCG allowed us to discriminate conjugates containing BCG within the conjugated monocyte from those that did not, on the basis of ds-Red fluorescent intensity (Fig. 5a,b). Antigen processing in phagocytic cells has previously been monitored using fluorescent molecule-labeled pathogens, where loss of fluorescent

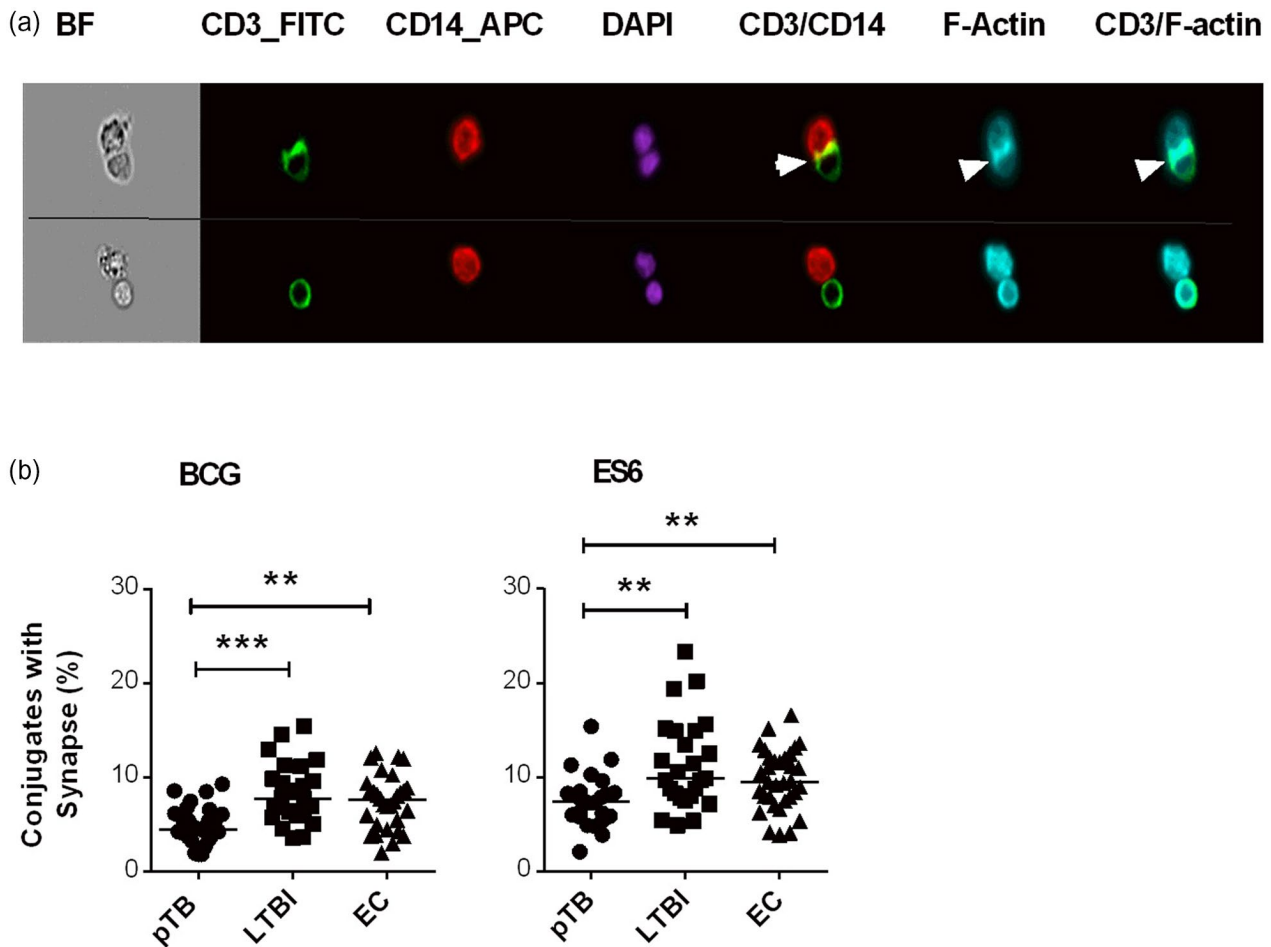


Fig. 3. TB antigen-induced T cell–monocyte conjugate formation. Peripheral blood mononuclear cells (PBMC) from patients with active pTB, latent TB infection (LTBI) individuals and endemic control (EC) groups were treated with 6-kDa early secreted antigenic target (ESAT 6) or ds-Red-expressing bacille Calmette–Guérin (BCG) for 6 h and T cell–monocyte conjugates were analyzed by imaging flow cytometer (IFC). (a) Image gallery from left to right showing; bright field (BF) images, T cells [CD3-fluorescein isothiocyanate (FITC)], monocytes (CD14-allophycocyanin) and nuclear image 4',6-diamidino-2-phenylindole (DAPI). The last three columns include: T cell–monocyte conjugates with polarized CD3/T cell receptor (TCR), F-actin and overlays of CD3/F-actin, consecutively, at the interface between T cell and monocyte conjugates (upper panel, white arrows). The corresponding images at lower panel presents T cell–monocyte conjugates with membrane contact without polarization of neither CD3/TCR nor F-actin at the interface between the two cells. (b) Scatter-plots showing the proportion of T cell–monocyte conjugates with synapse in cells from patients with active pTB (circles), LTBI (squares) and EC (triangles) in response to BCG or ES6. Horizontal bars represent median values and Kruskal–Wallis test with Dunn's multiple comparisons was used to assess differences among the three study groups: ** $P < 0.01$; *** $P < 0.001$.

signal has been associated with intracellular pathogen degradation [35,36]. Accordingly, we observed a significantly higher frequency of ds-Red-negative conjugates than the ds-Red-positive counterparts both in LTBI individuals and healthy EC, while the opposite was true in cells from patients with active pTB (Fig. 5c). Moreover, intergroup comparisons showed a significantly higher number of ds-Red-negative conjugates in LTBI individuals and EC than in patients with active pTB (Fig. 5c).

Having found that cells from control groups showed more ds-Red-negative conjugates, we evaluated its impact on NF- κ B nuclear translocation in the conjugating T cells.

Our data showed a significantly higher proportion of T cells displaying NF- κ B translocation when conjugated with ds-Red-negative monocytes compared to those T cells conjugated with ds-Red-positive monocytes in the same sample. Moreover, even though ds-Red-negative conjugates were fewer in PBMC from patients with active pTB, NF- κ B nuclear translocation was induced in conjugated T cells of this study group more frequently than in conjugated T cells those from LTBI individuals or healthy EC (Fig. 5d). Interestingly, NF- κ B nuclear translocation in T cells conjugated with ds-Red-positive monocytes did not show a significant difference among the study cohorts (Fig. 5d).

Discussion

Imaging flow cytometer (IFC) has proved to be a powerful tool in characterizing cell-cell interaction as well as monitoring intracellular localization of fluorescent-labeled molecules [37]. Our group has recently established a method using buffy coats of healthy blood donors as a source for PBMC, which enabled simultaneous monitoring

of antigen-induced T cell-monocyte conjugates and NF-κB nuclear translocation in T cells [26]. The method we established is based on the assumption that co-culturing live BCG with PBMC will result in phagocytosis of BCG by monocytes and the subsequent presentation of BCG-derived antigens to T cells present in the culture.

In our previous work, we performed kinetics experiments for up to 24 h to determine optimal culture

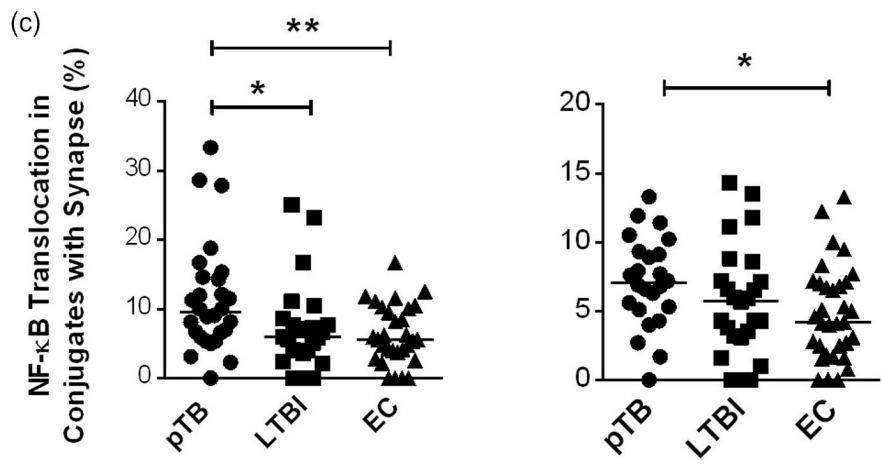
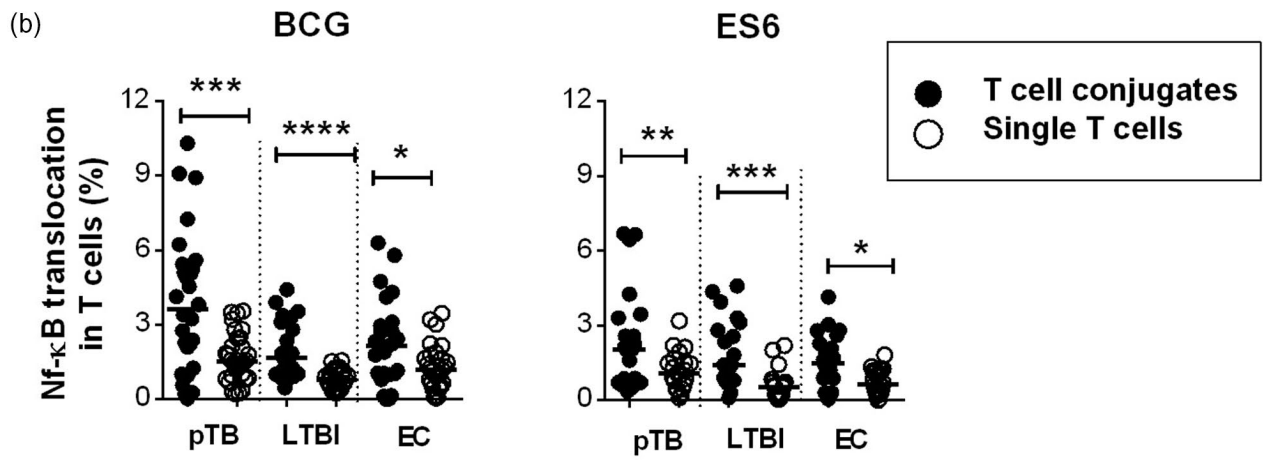
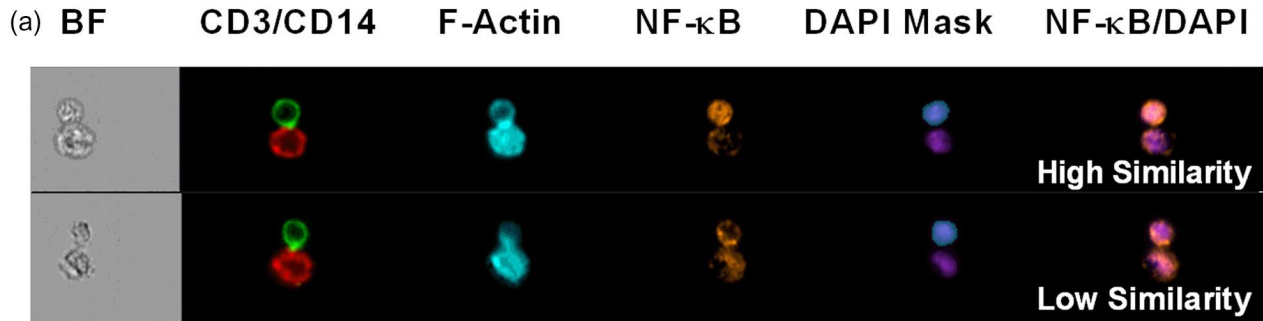


Fig. 4. Tuberculosis (TB) antigen-induced nuclear factor kappa B (NF- κ B) nuclear translocation in T cells. Peripheral blood mononuclear cells (PBMC) from patients with active pulmonary tuberculosis disease (pTB), latent TB infection (LTBI) individuals and endemic control (EC) groups were cultured as described above and NF- κ B nuclear translocation was assessed in responding T cells by imaging flow cytometer (IFC). (a) The first five columns of the image gallery from left to right are; bright field image, T cell–monocyte conjugates based on CD3 and CD14 signals, F-actin, NF- κ B and 4',6-diamidino-2-phenylindole (DAPI) nuclear mask, consecutively. The last column depicts NF- κ B and DAPI image overlays to locate whether NF- κ B is in the nucleus. Upper panel displays 'high similarity' between the two images, which is defined as 'NF- κ B nuclear translocation' while lower panel represents 'low similarity', which is defined as 'no translocation'. (b) Proportions of T cell conjugates (closed circles) and single T cells (open circles) displaying NF- κ B nuclear translocation in response to bacille Calmette–Guérin (BCG) or 6-kDa early secreted antigenic target (ESAT 6) stimulation in patients with pTB, LTBI individuals and EC group. (c') Plots presenting the rate of T cell–monocyte conjugates with established synapse and displaying NF- κ B nuclear translocation in cells of patients with active pTB (circles), LTBI individuals (squares) and EC (triangles) in response to BCG or ES6. Horizontal lines indicate median frequency. Results were analyzed using Wilcoxon's matched-pairs signed-rank test to compare median differences between single T cells with their counterparts of conjugated T cells of the same sample. The Kruskal–Wallis test with Dunn's multiple comparisons test was used to assess median differences among study cohorts: * $P < 0.05$; ** $P < 0.01$; *** $P < 0.001$; **** $P < 0.0001$.

condition. We found that 6-h incubation of PBMC with BCG resulted in adequate uptake of the pathogen by monocytes and the formation of T cell–monocyte conjugates. Longer incubation hours resulted in enhanced NF- κ B nuclear translocation in T cells, but T cell–monocyte conjugates frequency was severely reduced. The 6-h time-point was further validated using PBMC from a small cohort sample of active TB patients, obtained from the Norwegian Biobank for Infectious Disease. The results confirmed the feasibility of using stored PBMC for IFC analysis of conjugate formation and NF- κ B nuclear translocation. We then designed this larger study with well-defined groups in a disease-endemic country where we applied the method to identify, enumerate and characterize TB antigen reactive cells in clinical samples from patients with active pTB, LTBI individuals and healthy EC.

The immunological synapse (IS) is a specialized junction between a T cell and APC that is formed shortly after TCR recognition of its cognate peptide–MHC complex [20]. It is this cell surface recognition event that initiates an organized intracellular signaling cascade, resulting in T cell activation and effector function. Monocytes are among the critical components of the host immune system, both as effector cells *per se* and by representing the link to adaptive immune response as APC. In addition, monocytes are the precursors of monocyte-derived macrophages (MDM) and monocyte-derived dendritic cells (MDDC) [19].

The frequency of monocytes and lymphocytes as well as the ratio of monocytes-to-lymphocytes (M/L ratio) in peripheral blood is recognized as a valuable parameter in predicting the risk of active TB disease [32,38]. It has also been suggested that the increased M/L ratio is associated with changes in gene transcription in monocytes that may influence their anti-mycobacterial function [39]. In line with that reported by others, our data in the current study showed a significantly higher frequency of CD14⁺ monocytes with a corresponding increase in CD3⁺ T cells in patients with active pTB. This results in an increased M/L ratio

in PBMC from this study group compared to LTBI individuals or healthy EC. These findings also validated the performance of our IFC-based assay to correctly identify target cells in a heterogeneous cell population, as assessed previously by standard differential hematology and transcriptomic analysis.

Considering the elevated monocyte frequency, we initially anticipated more T cell–monocyte conjugates to be formed in PBMC from patients with active pTB upon co-culture. Surprisingly, our results indicated rather the opposite, with fewer T cell–monocyte conjugates in samples from active pTB cases compared to the controls. This observation was in line with studies that reported phenotypical and functional changes in the monocyte population, including reduced human leukocyte antigen D-related (HLA-DR), CD36 and CD86 expression during active TB [40,41]. Defective differentiation of monocyte to MDDC coupled with impaired function has also been reported in cells from pTB patients, as indicated by down-regulation of CD1a, MHC-II and CD80 expression [42]. Of note, these molecules are components of the antigen presentation machinery, and a reduction in expression would very probably lead to impaired antigen presentation to the T cell and initiation of adaptive immunity [43].

Upon BCG stimulation, we found more T cells with NF- κ B nuclear translocation in patients with active pTB than in the control groups. Although we did not differentiate between effector, naive or memory T cell phenotypes in our experiment, the finding is in agreement with previous studies that reported higher expression of activation markers, including CD38⁺HLA-DR⁺, in T cells from patients with active pTB [44]. One possible interpretation of this finding is thus that primed T cells display a quicker intracellular signaling response than that of naive T cells [45].

Infection-induced acquired immunity is accomplished by uptake, degradation, processing and presentation of antigen peptides, resulting in sensitization of the responding T cells. Antigen-derived peptides are generated by APCs through proteasome and lysosome degradation of the pathogen (reviewed in [46]). The process can be

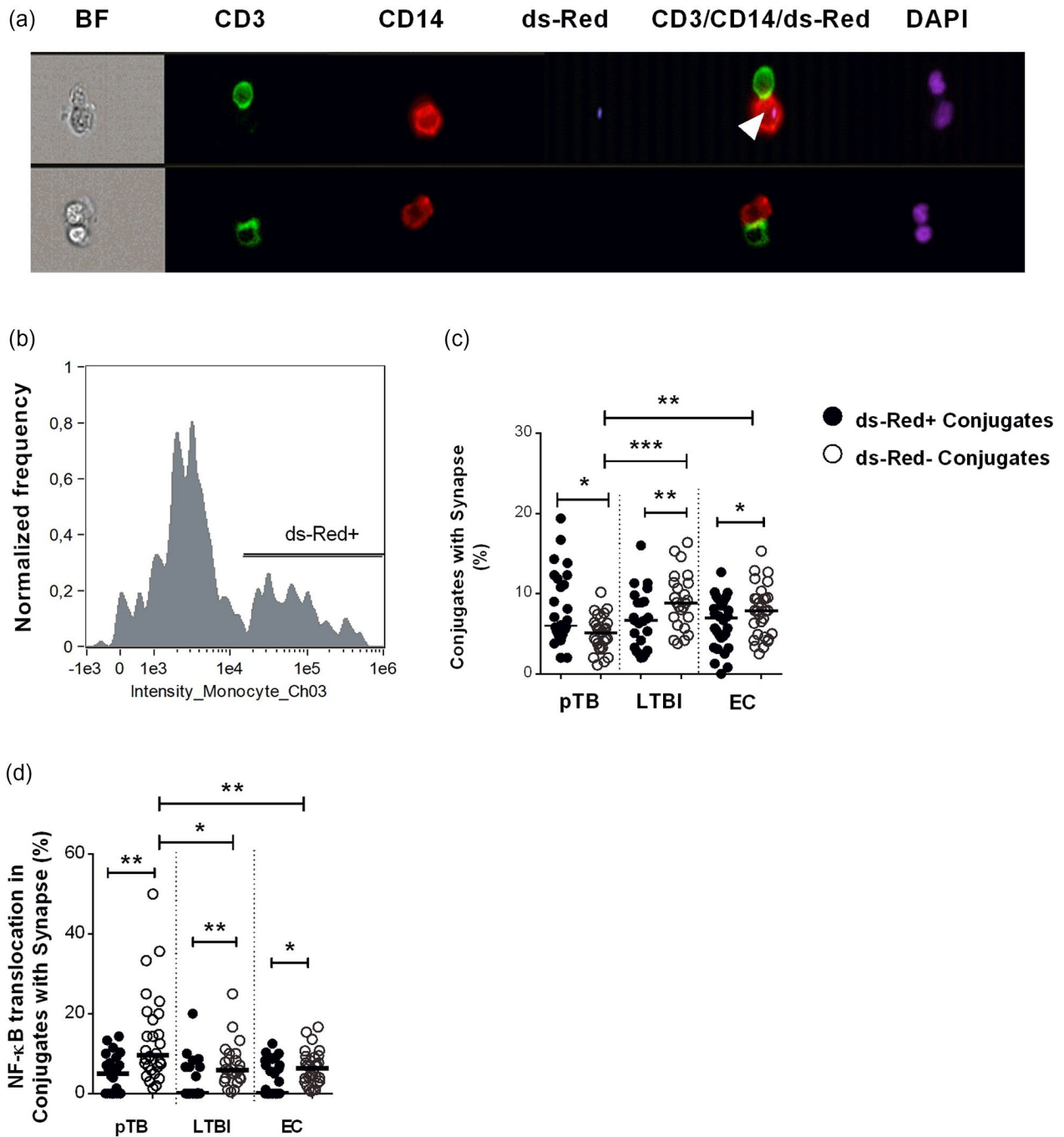


Fig. 5. ds-Red bacille Calmette–Guérin (BCG)-induced conjugate formation and nuclear factor kappa B (NF-κB) nuclear translocation. Cells from patients with pulmonary tuberculosis disease (pTB), latent TB infection (LTBI) individuals and endemic control (EC) group treated with ds-Red-expressing BCG for 6 h as described above. (a) Sample images displaying a T cell conjugated with ds-Red-positive monocyte (upper panel, white arrow) or ds-Red-negative monocyte (lower panel). (b) Representative histogram overlay for T cell–monocyte conjugates of BCG stimulated or unstimulated (filled gray) to define ds-Red-positive and ds-Red-negative T cell–monocyte conjugate subpopulations. (c) Scatter plot showing percentage of T cells displaying synapse when conjugated with ds-Red-positive monocytes (ds-Red⁺ conjugates, closed plots) or monocytes with no detectable ds-Red fluorescent signal (ds-Red⁻ conjugates, open plots) among patients with pTB, LTBI individuals and endemic controls (EC) group. (d) Proportion of T cells displaying NF-κB nuclear translocation when in conjugate with ds-Red⁺ (closed plots) or ds-Red⁻ monocytes (open plots). Horizontal bars represent median values and statistically significant differences between ds-Red⁺ and ds-Red⁻ conjugates were assessed by Wilcoxon's matched-pairs signed-rank test and Kruskal–Wallis test with Dunn's multiple comparisons was used to assess median differences among the three study groups: **P* < 0.05; ***P* < 0.01; ****P* < 0.001.

monitored using fluorescent molecule-labeled bacteria, where a dramatic loss in fluorescent signal is associated with intracellular pathogen degradation [35,47,48]. Taking advantage of the ability of IFC in monitoring fluorescently labeled molecules, we characterized BCG exposed T cell–monocyte conjugates further based on ds-Red fluorescence intensity. The results indicated that monocytes from active pTB cases process and present the antigen to T cells less efficiently, as reflected by fewer ds-Red-negative conjugates in this study population compared with controls. It is probable that the fewer ds-Red-negative conjugates in cells from pTB cases of BCG-stimulated samples could be explained, at least partly, by impaired monocyte function with regard to antigen processing and presentation [40].

One limitation of our assay was that it did not enable us to characterize ds-Red-negative conjugates further to discriminate between uninfected monocytes that formed conjugates spontaneously [49] from those that had taken up and degraded/processed the bacilli. However, the observation that a higher proportion of T cells displaying NF- κ B nuclear translocation when conjugated with ds-Red-negative monocytes than those conjugated with ds-Red-positives was compelling. In particular, it is intriguing that in T cells conjugated with ds-Red-negative monocytes, NF- κ B nuclear translocation was more pronounced. This finding indicated that the majority of ds-Red-negative conjugates contained infected monocytes that had processed the bacilli and presented antigen to the responding T cells. Among study groups, T cells conjugated with ds-Red-negative monocytes from patients with active pTB display NF- κ B nuclear translocation more frequently compared to T cells from LTBI individuals or healthy EC. Our results thus suggest that, despite a possibly reduced ability of monocytes in processing BCG antigens, the T cells were highly responsive once antigens became available for presentation on the surface of the monocyte. These findings are in line with studies that reported no deficiency of T cell function in patients with active TB, as evidenced by enhanced production of Th1 cytokines [6].

Infection of monocytes with ds-Red-expressing BCG allowed evaluation of the proportion of cells that have taken up and/or processed the BCG and characterization of those interacting with T cells. However, CD14 expression was greatly affected after incubation with live BCG (Supporting information, Fig. S2). This could explain the fewer T cell–monocyte conjugates we identified in BCG-stimulated cells compared with ESAT 6-stimulated pairs (Supporting information, Fig. S3). Loss of CD14 expression upon stimulation with BCG [50] and other bacteria such as *Escherichia coli* and Group B *Streptococci* [48] has also been reported previously. Considering other APC such as MDM and MDDC, as well as incorporating markers, which are less affected by stimulation condition, would help in addressing this challenge.

The use of BCG for stimulation enabled us to establish the assay in a facility where biosafety level 3 is not available as virulent *Mtb* strains. However, BCG does not contain the virulence-associated RD1 region of *Mtb*, which may result in variations in the functionality of the responding cells. It has been reported that peptide antigens are processed by APCs in the same way as intact bacteria [51]. ESAT 6 is a highly immunogenic *Mtb*-specific peptide encoded by the RD1 genomic region [52]. We thus included ESAT 6 in our experiment to assess *Mtb* specific response.

We have shown that IFC technology provide a statistically robust platform for studies of cell–cell interaction and co-localization of intracellular molecules. However, data generated from IFC are more complex, as IFC also includes fluorescent microscopy-related analysis. In addition, the high cost of purchasing the instrument makes it currently out of reach in most resource-limited settings. Hopefully, further improvements in the instrumentation and software will make the technology user friendly and affordable.

Overall, our data highlight the need for assessing multiple parameters representing immunological changes in innate and acquired immunity, rather than focusing only on T cell effector function in assessing the complex host response against TB. We thus believe that considering novel approaches, such as IFC, may contribute to the comprehensive overview necessary for the development of new and improved strategies in the fight against TB, including vaccine development and evaluation.

Acknowledgments

We would like to thank study volunteers for their participation and Alemayehu Kifle, Genet Amare, Hareg and Azeb Tarekegn for co-ordinating participant recruitment, sample collection and laboratory assistance. The study was supported by a Johs Svanholms grant, a Henrik Homans Mindes grant, University of Oslo, Quota scheme of the Norwegian State, the Norwegian Research Council (project number (grant no. 196386) and Armauer Hansen Research Institute (AHRI). AHRI receives core support from Norad, Sida and the government of Ethiopia.

Disclosures

The authors declare no conflicts of interest.

Author contributions

A. S., A. A., G. A., M. H. and M. A. conceived and designed the study; sample collection and preparation: M. H., E. A. and S. A; M. H. and G.A. performed the experiments,

acquired and analyzed the data; A. S., G. A., A. A. and M. A. interpreted the data and drafted the manuscript; M. H. critically reviewed the manuscript. All authors read and approved the manuscript. Primary mentor on the project: A. S.

References

- 1 WHO. Global tuberculosis report. Geneva, Switzerland: World Health Organization; 2017.
- 2 Pai M, Behr MA, Dowdy D *et al.* Tuberculosis. *Nat Rev Dis Primers* 2016; **2**:16076.
- 3 Cooper AM, Dalton DK, Stewart TA, Griffin J, Russell D, Orme I. Disseminated tuberculosis in interferon gamma gene-disrupted mice. *J Exp Med* 1993; **178**:2243–7.
- 4 Flynn JL, Chan J, Triebold KJ, Dalton DK, Stewart TA, Bloom BR. An essential role for interferon gamma in resistance to *Mycobacterium tuberculosis* infection. *J Exp Med* 1993; **178**:2249–54.
- 5 Majlessi L, Simsova M, Jarvis Z *et al.* An increase in antimycobacterial Th1-cell responses by prime-boost protocols of immunization does not enhance protection against tuberculosis. *Infect Immun* 2006; **74**:2128–37.
- 6 Mittrucker HW, Steinhoff U, Kohler A *et al.* Poor correlation between BCG vaccination-induced T cell responses and protection against tuberculosis. *Proc Natl Acad Sci USA* 2007; **104**:12434–9.
- 7 Fletcher HA, Filali-Mouhim A, Nemes E *et al.* Human newborn bacille Calmette–Guerin vaccination and risk of tuberculosis disease: a case–control study. *BMC Med* 2016; **14**:76.
- 8 Lu LL, Smith MT, Krystle K *et al.* IFN- γ -independent immune markers of *Mycobacterium tuberculosis* exposure. *Nat Med* 2019; **25**:977–87.
- 9 del Corral H, Paris SC, Marin ND *et al.* IFN γ response to *Mycobacterium tuberculosis*, risk of infection and disease in household contacts of tuberculosis patients in Colombia. *PLOS ONE* 2009; **4**:e8257.
- 10 Higuchi K, Harada N, Fukazawa K, Mori T. Relationship between whole-blood interferon-gamma responses and the risk of active tuberculosis. *Tuberculosis* 2008; **88**:244–8.
- 11 Dheda K, Schwander SK, Zhu B, Van Zyl-Smit RN, Zhang Y. The immunology of tuberculosis: from bench to bedside. *Respirology* 2010; **15**:433–50.
- 12 Zuniga J, Torres-Garcia D, Santos-Mendoza T, Rodriguez-Reyna TS, Granados J, Yunis EJ. Cellular and humoral mechanisms involved in the control of tuberculosis. *Clin Dev Immunol* 2012; **2012**:193923.
- 13 Liu CH, Liu H, Ge B. Innate immunity in tuberculosis: host defense vs pathogen evasion. *Cell Mol Immunol* 2017; **14**:963–75.
- 14 van Crevel R, Ottenhoff TH, van der Meer JW. Innate immunity to *Mycobacterium tuberculosis*. *Clin Microbiol Rev* 2002; **15**:294–309.
- 15 Kang DD, Lin Y, Moreno J-R, Randall TD, Khader SA. Profiling early lung immune responses in the mouse model of tuberculosis. *PLoS One* 2011; **6**:e16161.
- 16 Peters W, Ernst JD. Mechanisms of cell recruitment in the immune response to *Mycobacterium tuberculosis*. *Microbes Infect* 2003; **5**:151–8.
- 17 Skold M, Behar SM. Tuberculosis triggers a tissue-dependent program of differentiation and acquisition of effector functions by circulating monocytes. *J Immunol* 2008; **181**:6349–60.
- 18 Hohl TM, Rivera A, Lipuma L *et al.* Inflammatory monocytes facilitate adaptive CD4 T cell responses during respiratory fungal infection. *Cell Host Microbe* 2009; **6**:470–81.
- 19 Jakubzick CV, Randolph GJ, Henson PM. Monocyte differentiation and antigen-presenting functions. *Nat Rev Immunol* 2017; **17**:349–62.
- 20 Monks CR, Freiberg BA, Kupfer H, Sciaky N, Kupfer A. Three-dimensional segregation of supramolecular activation clusters in T cells. *Nature* 1998; **395**:82–6.
- 21 Grakoui A, Bromley SK, Sumen C *et al.* The immunological synapse: a molecular machine controlling T cell activation. *Science* 1999; **285**:221–7.
- 22 Delon J, Germain RN. Information transfer at the immunological synapse. *Curr Biol* 2000; **10**:R923–33.
- 23 Izzi G, Karjalainen K, Lanzavecchia A. The duration of antigenic stimulation determines the fate of naive and effector T cells. *Immunity* 1998; **8**:89–95.
- 24 Lucas PC, McAllister-Lucas LM, Nunez G. NF-kappaB signaling in lymphocytes: a new cast of characters. *J Cell Sci* 2004; **117**(Pt 1):31–9.
- 25 Tripathi P, Aggarwal A. NF-kB transcription factor: a key player in the generation of immune response. *Curr Sci Bangalore* 2006; **90**:519.
- 26 Habtamu M, Abebe M, Aseffa A, Dyrhol-Riise AM, Spurkland A, Abrahamsen G. *In vitro* analysis of antigen induced T cell–monocyte conjugates by imaging flow cytometry. *J Immunol Methods* 2018; **460**:93–100.
- 27 Abadie V, Badell E, Douillard P *et al.* Neutrophils rapidly migrate via lymphatics after *Mycobacterium bovis* BCG intradermal vaccination and shuttle live bacilli to the draining lymph nodes. *Blood* 2005; **106**:1843–50.
- 28 Wang L, Hüchelhoven A, Hong J *et al.* Standardization of cryopreserved peripheral blood mononuclear cells through a resting process for clinical immunomonitoring – development of an algorithm. *Cytometry Part A* 2016; **89**:246–58.
- 29 Havixbeck JJ, Wong ME, More Bayona JA, Barreda DR. Multi-parametric analysis of phagocyte antimicrobial responses using imaging flow cytometry. *J Immunol Methods* 2015; **423**:85–92.
- 30 Ahmed F, Friend S, George TC, Barteneva N, Lieberman J. Numbers matter: quantitative and dynamic analysis of the formation of an immunological synapse using imaging flow cytometry. *J Immunol Methods* 2009; **347**:79–86.
- 31 George TC, Fanning SL, Fitzgerald-Bocarsly P *et al.* Quantitative measurement of nuclear translocation events using similarity analysis of multispectral cellular images obtained in flow. *J Immunol Methods* 2006; **311**:117–29.
- 32 Naranbhai V, Kim S, Fletcher H *et al.* The association between the ratio of monocytes: lymphocytes at age 3 months and risk

- of tuberculosis (TB) in the first two years of life. *BMC Med* 2014; **12**:120.
- 33 Wang J, Yin Y, Wang X *et al.* Ratio of monocytes to lymphocytes in peripheral blood in patients diagnosed with active tuberculosis. *Braz J Infect Dis* 2015; **19**:125–31.
- 34 Dustin ML, Choudhuri K. Signaling and polarized communication across the T cell immunological synapse. *Annu Rev Cell Dev Biol* 2016; **32**:303–25.
- 35 Li W, Houston KD, Houston JP. Shifts in the fluorescence lifetime of EGFP during bacterial phagocytosis measured by phase-sensitive flow cytometry. *Sci Rep* 2017; **7**:40341.
- 36 Gille C, Spring B, Tewes L, Poets CF, Orlikowsky T. A new method to quantify phagocytosis and intracellular degradation using green fluorescent protein-labeled *Escherichia coli*: comparison of cord blood macrophages and peripheral blood macrophages of healthy adults. *Cytometry A* 2006; **69**:152–4.
- 37 McFarlin BK, Gary MA. Flow cytometry what you see matters: enhanced clinical detection using image-based flow cytometry. *Methods* 2017; **112**:1–8.
- 38 La Manna MP, Orlando V, Dieli F *et al.* Quantitative and qualitative profiles of circulating monocytes may help identifying tuberculosis infection and disease stages. *PLOS ONE* 2017; **12**:e0171358.
- 39 Naranbhai V, Fletcher HA, Tanner R *et al.* Distinct transcriptional and anti-mycobacterial profiles of peripheral blood monocytes dependent on the ratio of monocytes: lymphocytes. *EBioMedicine* 2015; **2**:1619–26.
- 40 Sakhno LV, Shevela EY, Tikhonova MA, Nikonov SD, Ostanin AA, Chernykh ER. Impairments of antigen-presenting cells in pulmonary tuberculosis. *J Immunol Res* 2015; **2015**:14.
- 41 Sánchez MD, García Y, Montes C *et al.* Functional and phenotypic changes in monocytes from patients with tuberculosis are reversed with treatment. *Microbes Infect* 2006; **8**:2492–500.
- 42 Rajashree P, Krishnan G, Das SD. Impaired phenotype and function of monocyte derived dendritic cells in pulmonary tuberculosis. *Tuberculosis* 2009; **89**:77–83.
- 43 Lee J, Tam H, Adler L, Ilstad-Minnihan A, Macaubas C, Mellins ED. The MHC class II antigen presentation pathway in human monocytes differs by subset and is regulated by cytokines. *PLOS ONE* 2017; **12**:e0183594.
- 44 Rodrigues DSS, Medeiros EAS, Weckx LY, Bonnez W, Salomão R, Kallas EG. Immunophenotypic characterization of peripheral T lymphocytes in *Mycobacterium tuberculosis* infection and disease. *Clin Exp Immunol* 2002; **128**:149–54.
- 45 Ericsson PO, Orchansky PL, Carlow DA, Teh HS. Differential activation of phospholipase C-gamma 1 and mitogen-activated protein kinase in naive and antigen-primed CD4 T cells by the peptide/MHC ligand. *J Immunol* 1996; **156**:2045–53.
- 46 Blum JS, Wearsch PA, Cresswell P. Pathways of antigen processing. *Annu Rev Immunol* 2013; **31**:443–73.
- 47 Schreiner L, Huber-Lang M, Weiss ME, Hohmann H, Schmolz M, Schneider EM. Phagocytosis and digestion of pH-sensitive fluorescent dye (Eos-FP) transfected *E. coli* in whole blood assays from patients with severe sepsis and septic shock. *J Cell Commun Signal* 2011; **5**:135–44.
- 48 Gille C, Leiber A, Mundle I *et al.* Phagocytosis and postphagocytic reaction of cord blood and adult blood monocyte after infection with green fluorescent protein-labeled *Escherichia coli* and group B Streptococci. *Cytometry B Clin Cytometry* 2009; **76**:271–84.
- 49 Brossard C, Feuillet V, Schmitt A *et al.* Multifocal structure of the T cell–dendritic cell synapse. *Eur J Immunol* 2005; **35**:1741–53.
- 50 Shey MS, Hughes EJ, de Kock M *et al.* Optimization of a whole blood intracellular cytokine assay for measuring innate cell responses to mycobacteria. *J Immunol Methods* 2012; **376**:79–88.
- 51 Bhardwaj V, Colston MJ. The processing and presentation of mycobacterial antigens by human monocytes. *Eur J Immunol* 1988; **18**:691–6.
- 52 Sorensen AL, Nagai S, Houen G, Andersen P, Andersen AB. Purification and characterization of a low-molecular-mass T-cell antigen secreted by *Mycobacterium tuberculosis*. *Infect Immun* 1995; **63**:1710–7.

Supporting Information

Additional supporting information may be found in the online version of this article at the publisher's web site:

Fig. S1. Antigen induced NF- κ B translocation in T cells conjugated with monocytes analyzed by Imaging flow cytometer.

Fig. S2. Effect of antigen stimulation on single CD14⁺ monocytes.

Fig. S3. Effect of TB antigens on T cell–monocyte conjugate formation.